Viscoplastic-Elastic Modeling of Tubular Blown Film Processing

The blown film process has been modeled through the transition from liquidlike to solidlike behavior at the freeze line. A new constitutive equation has been developed that, when incorporated into the the kinematic and dynamic equations that describe the process, for the first time yields qualitatively correct predictions of all process variables. It is suggested that the demarcation between liquidlike behavior and solidlike behavior be altered from the conventional, kinematically based constraint, $dr/dz = 0$, to a rheologically based constraint, the plastic-elastic transition (PET). The results are qualitive in nature since the material is modeled as an elastic solid above the PET instead of as a viscoelastic material. The model is tested using the polystyrene data of Gupta (1981).

Bangshu Cao
Gregory A. Campbell
Polymer Fabrication and Properties Laboratory
Department of Chemical Engineering
Clarkson University
Potsdam NY 13676

Introduction

Tubular film blowing is one of the most important industrial techniques for the production of thin, biaxially oriented films. As a result, it has received substantial attention in the literature. The process, represented in Figure 1, involves extruding thermoplastic melts through an annular die followed by biaxial stretching of the polymer bubble with intensified cooling.

Our long-term goal in this laboratory is to develop a method for predicting the physical properties of the formed film, assuming that the properties will not change significantly after the polymer has essentially cooled to room temperature. This goal was defined to try to improve the efficiency of resin and process development. It is not uncommon today in new product or process development to make blown film from literally tons of experimental resin to determine the effect of process parameters on film properties. This situation is in part due to the lack of a modeling simulation technique that adequately describes the process from the die to the nip rolls. We feel that the polymer is stretched up to the freeze line and then the frozen-in strain partially relaxes as the polymer continues to cool between the freeze line and the nips. If this is an appropriate description, it is important to extend the simulation through and above the freeze line because the time it takes to cool the polymer will influence the biaxial structure development and therefore the final physical properties of the film. We also feel that a rheological model that will quantitatively fit the experimental process data without altering the measured process parameters needs to be developed. This paper develops a possible approach which may, when refined, ultimately accomplish these goals.

The process is generally started by capping an annular extrudate and sealing the formed bubble with the nip rolls. Air is then introduced into the bubble; and the nip rolls and the extruder are increased in speed until the process requirements are met. Industrial experience dictates that the product properties are also a function of the frost line height, which is in reality an observation of a change in refractive index of the polymer. In polyethylene, it is often thought to be associated with crystallization; however, a frost line comes and goes when producing film from amorphous polystyrene. The frost line height and the shape of the bubble are influenced by the velocity and temperature of the air that is applied to the exterior of the bubble by one or more annular jets produced by an air ring, as shown by Cao and Campbell (1989), and influenced by the temperature distribution across the film, as indicated by Cao et al. (1989).

Essentially all literature models and simulations of the blown film process stop at the freeze line. The freeze line, as defined by Pearson and Petrie (1970b), is a kinematic constraint on the film blowing process, the point where the film is parallel to the centerline of the bubble, which more or less corresponds to the observed frost line. Although observable strain rate ceases at the freeze/frost line for many resins, the temperature of the polymer may decrease as much as 130 K as it moves from the freeze line to the nip rolls.

The polymer is considered to be a complex liquid at the die which undergoes biaxial stretching and cooling. The polymer

Correspondence concerning this paper should be addressed to G. A. Campbell.

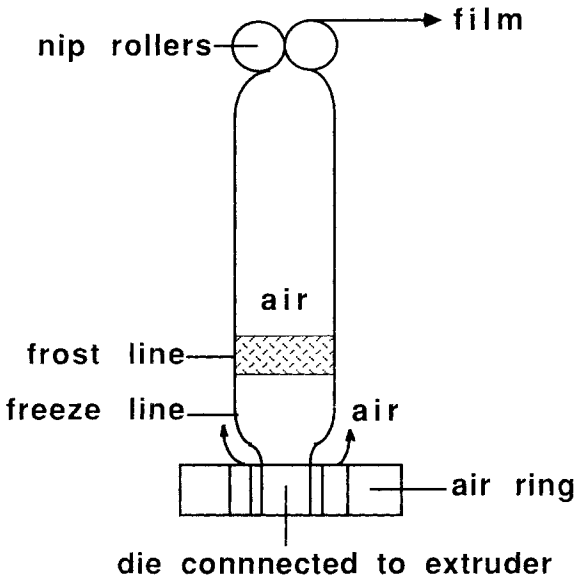

Figure 1. Blown film line.

then changes to a solidlike state in the vicinity of the freeze/frost line. As a viscoelastic material, polymers remember their stress-strain-temperature history. Creep recovery during the time it takes to cool the polymer would be expected to affect any properties that are structure dependent. Gupta (1981) found that the freeze line for polystyrene was 40–60 K above the glass transition temperature. It would be expected that substantial changes in structure occur during the time that the polystyrene polymer was cooled approximately 130 K to room temperature. The basic assumption used in the present analysis is that the polymer is stretched up to the freeze line and then the frozen-in orientation partially relaxes, as the polymer continues to cool as it moves through the freeze zone to the nips. To test this concept, it will be necessary to extend the simulation through and above the freeze line because the time it takes to cool the polymer will influence the biaxial structure development and therefore the final physical properties of the film.

Since the classical analysis of Pearson and Petrie (1970a, b, c) first present a theoretical framework for understanding the blown film process from the view point of fluid mechanics, various rheological models have been incorporated in simulations, such as the Newtonian model by Petrie (1975), the power law model by Han and Park (1975) and the crystallization model by Kanai and White (1985), the Maxwell-model by Petrie (1973) and Wagner (1976), the Leonov model by Luo and Tanner (1985), and the Marrucci model by Cain and Denn (1988). All of these simulations were reported from the die to the conventional freeze line. It is understood that a liquidlike model cannot be used to describe the behavior of the film above the freeze line, since the polymer becomes solidlike. However, a solidlike model, for example the Hookean model, should not be used in conjunction with a liquidlike model unless there is a natural shift between the two models. In this paper, we propose a model that makes such a natural transition.

Process Analysis

In the course of developing a model for the entire simulation from the die to the nip rolls, we at first attempt to introduce the classical Bingham model into the analysis, since a yield stress can be used to explain why there is no deformation above the freeze line even though there are still stresses present in the film (Campbell and Cao, 1987). The Bingham model produced a straight bubble contour above the freeze line, but rheologically it was too simple. As a result, the process parameters such as the take-up force or the inflation pressure had to be changed by a factor of 2 or 3 to make the model fit the literature data. Since there is no time-derivative of stress in the Bingham model, the transient characteristics of the blown film process were not described by the model.

This led us to consider the development of a new model by introducing the concept of yield into viscoleastic models. Below the freeze line, the polymer is considered to be a viscoelastic fluid and above the freeze line it is assumed to be an elastic solid. This is an oversimplification since the polymers are actually viscoelastic solids. After evaluating several models, we observed that the bubble shape above the freeze line was still predicted to either collapse or expand rapidly, similar to other viscoelastic models. A model sensitivity analysis indicated that the modulus based on the reported data was not large enough to maintain the bubble radius at a reasonably constant value above the freeze line. The need for a larger effective modulus in the vicinity of the freeze line led us to consider strain hardening effects, which may cause a significant increase in the modulus and viscosity of polymers undergoing extensional flow. We quantified the strain hardening effects using the concept of polymer chain alignment. In this preliminary analysis, our newly designed model is neither based on molecular arguments, nor on a strict derivation from continuum mechanics. Instead, the model is a phenomenological modification of the Maxwell model. The following sections explain in detail the proposed model that appears to provide many of the correct trends in the vicinity of the freeze line when incorporated in the simulation of the blown film process.

Strain hardening

We would like to incorporate a quantitative prediction in our constitutive equation of the effect of strain hardening. In uniaxial and biaxial elongation, the stress may increase very rapidly in excess of the level predicted by the theory of linear viscoelasticity. Increases in stress of two or three orders of magnitude occurring at some time after the start of the motion at a constant deformation rate have been reported by Meissner (1971). This phenomenon is often called strain hardening. It is not seen in steady shear, since the polymer chains are essentially in a neutral alignment in a shear field. It is widely accepted that strain hardening is most likely due to the alignment of molecules in the direction(s) of stretching. To characterize the extent of the alignment, Larson (1988) suggested using the following criteria:

$$I_1 - I_2 > 0 \quad \text{strongly aligning}$$

$$I_1 - I_2 = 0 \quad \text{neutrally aligning}$$

$$I_1 - I_2 < 0 \quad \text{weakly aligning}$$

where I_1 and I_2 are the first and the second invariants of the Finger tensor, $\mathbf{C}^{-1}(t, t')$.

$$I_1 = tr\mathbf{C}^{-1}(t, t') \tag{1}$$

$$I_2 = tr\mathbf{C}(t, t') \tag{2}$$

For an incompressible fluid, the second invariant of the Finger tensor is equal to a trace of the Cauchy-Green tensor, $\mathbf{C}(t, t')$, an inverse of the Finger tensor. The measure, $I_1 - I_2$, was called alignment strength. According to these criteria, uniaxial extension is strongly aligning due to molecules orienting along a single axis. Biaxial extension is thought to be weakly aligning, since the molecules are stretched in two perpendicular directions. Planar extension and simple shear fall into the category of neutral alignment, because both have a neutral axis, with stretching and compression along the other two axes. As pointed out by Larson (1988), most viscoelastic models, such as the Giesekus (1982) and PTT (Phan-Tanner, 1977) models, are not sensitive to alignment strength. Larson's definition of alignment strength yields a negative alignment strength in a biaxial elongational flow. Since the molecular alignment generally increases with the development of strain in both uniaxial and biaxial extension, we feel that a definition of positive definite alignment strength is physically more appealing and mathematically more convenient to incorporate in a constitutive equation. In the course of defining a positive definite alignment strength, we do not simply impose an absolute value sign on the Larson alignment strength, $|I_1 - I_2|$, because it would produce the same alignment strength for both uniaxial and equal-biaxial extension for equivalent strains. Experiments show strong alignment of molecules in uniaxial extension and weaker alignment in equal-biaxial extension. This leads us to seek a model that can predict the strain hardening for both uniaxial and biaxial extension through an application of alignment strength. Starting with the concepts introduced by Larson, we introduce an alternative definition of alignment strength that is subsequently used in our constitutive model:

$$\psi = |I_1 - I_2| \frac{I_1}{I_2} \tag{3}$$

The newly defined alignment strength is positive definite. Nonequivalent values of the alignment strength for strain in uniaxial and equal-biaxial extension are due to the term, I_1/I_2. As illustrated in Figure 2, the alignment strength based on this definition is much stronger for uniaxial extension than that for equal-biaxial extension. Larson's alignment strength in uniaxial extension is also plotted against strain, in Figure 2. Although our definition of the alignment strength is different from Larson's mathematically, we believe they are physically consistent. In fact, we have used Larson's physical concepts—strong alignment in uniaxial elongational flow, neutral alignment in planar and shear flow, and weak alignment in biaxial elongational flow—to develop our model.

Plastic-elastic transition

In the blown film process the stretch ratios in the radial and machine directions can be up to 8:1 and 80:1, respectively. This is well beyond the traditional limits of linear viscoelasticity. Therefore we propose that the total deformation the polymer material experiences may be decomposed into a recoverable elastic part and unrecoverable plastic part. We define a plastic-elastic transition zone (PET). Below the PET, plastic deformation is expected to dominate. Above the PET, the material is essentially solidified such that elastic deformation would be expected to dominate. In our analysis the freeze line and the PET do not necessarily coincide. The demarcation between liquidlike behavior and solidlike behavior is altered from the conventional kinematically based constraint to a rheologically based constraint, the plastic-elastic transition.

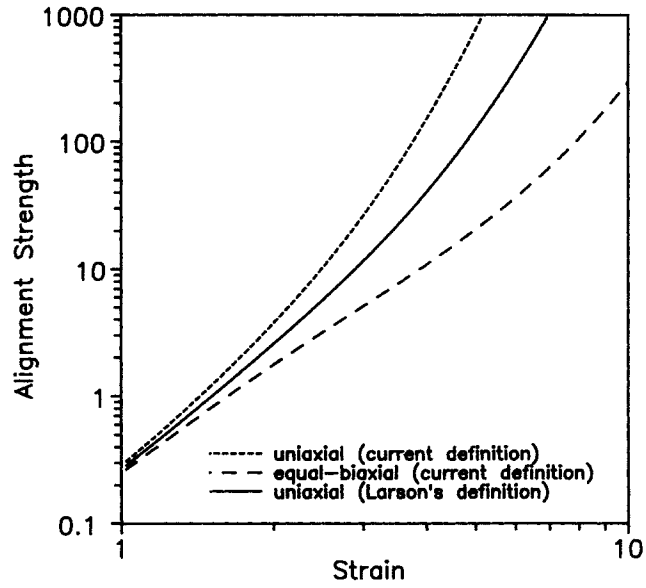

Figure 2. Alignment strength, ψ, in elongational flows.

To accomplish this, we used a yield stress as the criterion. The concept of yield in polymers is different from that in metals and has been somewhat controversial for past few years. Using the reasoning of Hartnett and Hu (1989), we believe that yield stress in the blown film process may be considered an engineering reality. Yielding behavior has been investigated for both partially crystallized polymers, reported by Hartmann and Cole (1983) and Chow (1987), and amorphous polymers, reported by Beatty and Weaver (1978) and Chow (1987). In the present study, yield stress is treated as a function of temperature, strain rate, and alignment strength. We use the term "effective yield stress" to distinguish it from conventional yield stress in the Bingham plastic model. In the blown film process, the yield stress is very small at the die, since the temperature is high and the alignment strength is low. But near the PET, the effective yield stress increases rapidly due to decreasing temperature and increasing alignment strength. In the present study, the effective yield stress is defined specifically as:

$$Y_{eff} = Y\zeta \tag{4}$$

$$\zeta = C_h \int_{-\infty}^{t} \sqrt{\Pi_D}\psi \exp\left(-\frac{(t - t')}{\lambda_{eff}}\right) dt' \tag{5}$$

where Y is the conventional yield stress, a function of temperature only; C_h is an empirical constant; $\sqrt{\Pi_D}$ is the second invariant of deformation rate tensor; and ψ is the alignment strength defined in Eq. 3. The structure memory function ζ, Eq. 5, is introduced to quantify the combined effects of alignment and elongation rate on yield stress. Analogous to the conventional memory function, a factor, $\exp[-(t - t')/\lambda_{eff}]$ is inserted into the integral to account for the relaxation of the alignment strength. According to Eq. 5, the structure memory function is zero for an undeformed material. The introduction of $\sqrt{\Pi_D}$ into the structure memory function, ζ, is to lead to a relaxation time

analogous to the one defined in the White-Metzner (1963) model, which possesses the characteristic of thermodynamic irreversibility. The effective relaxation time is discussed in the next section. Rapid growth of the alignment strength due to polymer orientation causes the structure memory function to increase very rapidly. We feel that the use of a yield criterion is physically reasonable, since in the blown film process there appears to be no measurable strain rate above the frost line, even though there are relatively large stresses in the two stretching directions.

Effective relaxation time

Blowing film is essentially a transient process with respect to stress growth. It is known that it generally takes only 1–4 s for a material element to move from the die to the freeze line. During this time a stress field is built up inside the polymer film. Most experimental results indicate that the viscosity of polymer melts increases at least one order of magnitude from the onset of motion until reaching a kinematic equilibrium in a period of about two seconds. The generalized Newtonian models were not able to describe the stress growth phenomenon, since there is no time-derivative involved in those constitutive equations. Therefore, it may not be proper to use equilibrium values of the material functions based on those models in the simulation. Viscoelastic models contain a time-derivative of stress, but some, such as the Maxwell model, are thermodynamically reversible, as pointed by Larson (1988). At infinitely large deformation rate, the Maxwell model reduces to the elastic limit. Other models which address irreversible flow are rheologically independent of the alignment strength, such as the White-Metzner model. In order to develop a constitutive equation that is time dependent, thermodynamically irreversible, and incorporates strain hardening, we define an effective relaxation time that is associated with the time-derivative of stress.

To achieve this goal, an effective modulus is defined in a similar way to the effective yield stress:

$$G_{eff} = G(1 + \zeta) \tag{6}$$

where G is the conventional modulus, a function of temperature only. The effective modulus is enhanced by increasing alignment strength and deformation rate as a result of elongational flow. Combining the viscosity, effective yield stress, and effective modulus leads to effective relaxation time:

$$\lambda_{eff} = \frac{\eta_{eff}}{G_{eff}} \tag{7}$$

$$\eta_{eff} = \frac{\eta}{1 - \dfrac{Y_{eff}/\sqrt{3}}{\sqrt{\Pi_\tau}}} \tag{8}$$

Equation 7 is analogous to the conventional definition of relaxation time, a ratio of viscosity to modulus. Equation 8 is analogous to the definition of viscosity in the Bingham model. Since the effective yield stress and modulus are functions of deformation rate and the alignment strength as defined in Eqs. 4–6, the effective relaxation time is also dependent on deformation rate and alignment strength. At very high deformation rates, the effective relaxation time approaches zero, similar to White-Metzner model behavior. No matter how fast the deformation occurs, stress relaxation always exists immediately after the deformation and the model will never reduce to the elastic limit, $\sigma = GE$. Therefore, the model is thermodynamically irreversible. The effective relaxation time depends strongly on the alignment strength, especially near the plastic-elastic transition zone where the relaxation time approaches infinity due to the denominator in Eq. 8 approaching zero. An infinitely large relaxation time implies that the plastic deformation is terminated and elastic deformation will then dominate.

Kinematics and dynamics

The kinematic and dynamic analysis of the blown film process was developed by Pearson and Petrie (1970b) using a surface coordinate system, Figure 3. The three principle directions—machine direction, normal direction, and circumferential direction—are denoted using 1, 2, and 3, respectively. The origin of the coordinate system is located on the inner surface of the film and "flows" downstream with the movement of the film. The deformation rate tensor in this coordinate system can be expressed in term of the film velocity, v, the bubble radius, r, the film thickness, h, the axial angle of the film contour, θ, and the distance from the die, z:

$$\mathbf{D} = v\cos\theta \begin{bmatrix} \dfrac{1}{v}\dfrac{dv}{dz} & 0 & 0 \\ 0 & \dfrac{1}{h}\dfrac{dh}{dz} & 0 \\ 0 & 0 & \dfrac{1}{r}\dfrac{dr}{dz} \end{bmatrix} \tag{9}$$

The dynamic analysis of the blown film process is more appropriately called a static analysis, since the inertial term is ignored in the analysis due to the low Reynolds number for the polymer flow in the blown film process. The static equilibrium equations in the two stretching directions were established by Pearson and Petrie (1970b)

$$2\pi rh\sigma_{11}\cos\theta + \pi\Delta p(r_f^2 - r^2) = F_z \tag{10}$$

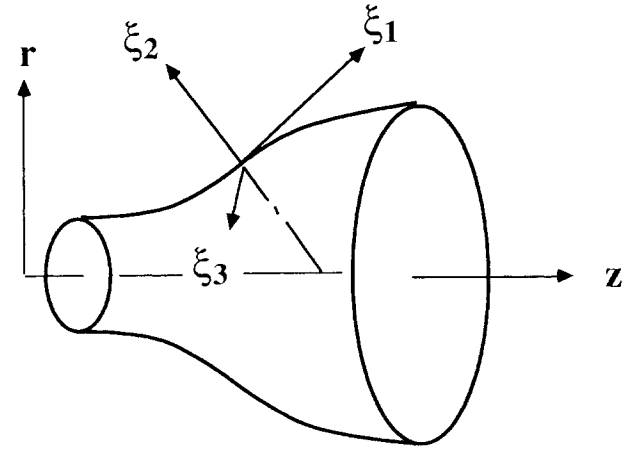

Figure 3. Surface coordinates.

$$\frac{h\sigma_{11}}{R_L} + \frac{h\sigma_{33}}{R_H} = \Delta p \tag{11}$$

$$R_L = -\frac{\sec^3\theta}{d^2r/dz^2} \tag{12}$$

$$R_H = r \sec\theta \tag{13}$$

The effects of gravity and surface tension are neglected here, but discussed by Petrie (1975).

Constitutive equations

Our constitutive model is cast as:

$$\begin{cases} \lambda_{eff}\tau_{[1]} + \tau = 2\eta_{eff}\mathbf{D} & \text{if } \sqrt{\Pi_\tau} > Y_{eff}/\sqrt{3} \\ \tau = 2G_{eff}\mathbf{E} & \text{if } \sqrt{\Pi_\tau} < Y_{eff}/\sqrt{3} \end{cases} \tag{14}$$

The first part of the above equation is a modified Maxwell model and the second part is a modified Hookean model. We utilize the convective derivative, $\tau_{[1]}$, as defined by Bird et al. (1977). The effective relaxation time, λ_{eff}, effective viscosity, η_{eff}, effective modulus, G_{eff} and effective yield stress, Y_{eff}, are defined in Eqs. 4–8. A spatial coordinate system is used for the deformation rate tensor, **D**, and a material coordinate system is used for the strain tensor, **E**, defined as the Hencky strain above the PET. The reference configuration for the strain tensor is the unstressed state of the material. The relaxation time in our constitutive model is a function of the alignment strength, which depends on the Finger tensor, $\mathbf{C}^{-1}$. The Finger tensor, which was used by Petrie (1975), Wagner (1978) and Winter (1982) for the blown film process, is cast as:

$$\mathbf{C}^{-1}(t, t') = \begin{bmatrix} \dfrac{v^2(t)}{v^2(t')} & 0 & 0 \\ 0 & \dfrac{h^2(t)}{h^2(t')} & 0 \\ 0 & 0 & \dfrac{r^2(t)}{r^2(t')} \end{bmatrix} \tag{15}$$

The model shifts from the liquidlike to the solidlike behavior at the PET when the effective yield stress is equal to the square root of three times the second invariant of the stress tensor, that is, the Vohn-Mises yield condition (Hill, 1950) is satisfied. Under different conditions, the proposed model will translate to several different models: If the structure memory function ζ is equal to zero, the governing equation reduces to the original Maxwell model. If the relaxation time is equal to zero, the governing equation reduces to the Bingham model. If both the structure memory function ζ and the relaxation time are equal to zero, the governing equation reduces to the Newtonian model. Finally, if the yield stress is always larger than the imposed stress the constitutive model reduces to the Hookean model.

System equations and boundary conditions below the PET

Upon substituion of the irreversible portion of the constitutive equation, Eq. 14, and the deformation rate tensor, Eq. 9, into the total stress tensor:

$$\sigma_{ij} = -p\delta_{ij} + \tau_{ij} \tag{16}$$

we find the following governing equations below the PET:

$$\sigma'_{11} - 2\sigma_{11}\frac{v'}{v} + 2p\left(\frac{h'}{h} - \frac{v'}{v}\right) + \frac{\sigma_{11}}{\lambda_{eff}v\cos\theta} = \frac{2\eta_{eff}}{\lambda_{eff}}\left(\frac{v'}{v} - \frac{h'}{h}\right) \tag{17}$$

$$p' - 2p\frac{h'}{h} + \frac{p}{\lambda_{eff}v\cos\theta} = \frac{2\eta_{eff}}{\lambda_{eff}}\frac{h'}{h} \tag{18}$$

$$\sigma'_{33} - 2\sigma_{33}\frac{r'}{r} + 2p\left(\frac{h'}{h} - \frac{r'}{r}\right) + \frac{\sigma_{33}}{\lambda_{eff}v\cos\theta} = \frac{2\eta_{eff}}{\lambda_{eff}}\left(\frac{r'}{r} - \frac{h'}{h}\right) \tag{19}$$

where the prime denotes d/dz.

Recognizing that

$$r' = \tan\theta \tag{20}$$

we can rewrite Eq. 11 as:

$$\theta' = \frac{\sigma_{33}}{r\sigma_{11}} - \frac{\Delta p}{\cos\theta h\sigma_{11}} \tag{21}$$

With the aid of Eq. 21, the axial force balance, Eq. 10 is recast as a differential equation:

$$\sigma'_{11} = \frac{r'}{r}\left(\sigma_{33} - \sigma_{11}\right) - \frac{h'}{h}\sigma_{11} \tag{22}$$

The energy balance as addressed by Petrie (1974, 1975), and Han and Park (1975) can be represented as:

$$\rho C_p h v\cos\theta T' = -U(T - T_a) - \lambda\epsilon(T^4 - T_a^4) \tag{23}$$

where T_a is the temperature of the cooling air; ρ the density; C_p the specific heat; U is the heat transfer coefficient due to convection, assumed to be a constant in our analysis for simplicity; λ is the Stefan-Boltzmann constant; and ϵ is the emissivity of the film. Luo and Tanner (1985), and Cain and Denn (1988), added a dissipation term in the energy balance. In the present study the dissipation term is considered to be very small and thus can be ignored. Kanai and White (1983) also added another term to the energy balance to account for the latent heat in crystalline polymers. Since the present study is focused on amorphous polymers only, we do not need to include this term.

The system equations for the blown film process based on our viscoplastic-elastic constitutive model are Eqs. 17–23, seven differential equations. Seven unknowns, σ_{11}, σ_{33}, p, r, h, θ, and T are obtained by solving the system equations simultaneously. The velocity, v, is an unknown in the system equations, but it can be eliminated by using an equation of continuity:

$$\pi rhv\rho = \dot{m} \tag{24}$$

where, the polymer flow rate, $\dot{m}$, is a constant for steady state.

Differentiating Eq. 22 and assuming a constant density of the polymer leads to

$$\frac{v'}{v} + \frac{h'}{h} + \frac{r'}{r} = 0. \tag{25}$$

Equation 25 has been used to eliminate v' in the system equations.

Seven boundary conditions are associated with the system equations. Four of them at the die are:

$$r|_{die} = r_0,$$
$$h|_{die} = h_0,$$
$$T|_{die} = T_0,$$
$$\sigma_{11}|_{die} = \frac{F_z + \pi\Delta p(r_0^2 - r_f^2)}{2\pi h_0 r_0 \cos\theta_0}$$

where the subscript 0 refers to the die. Since the initial angle, θ_0, and blow-up ratio are unknowns, we do not really know $\sigma_{11}|_{die}$. Therefore, we take θ_0 as a parameter, as have been done previously by Luo and Tanner (1986) and Cain and Denn (1988). At the PET, we shift governing equations from the modified Maxwell model to the modified Hookean model. Three more boundary conditions are the used: r, v, and θ change continuously through the shift of the governing equations. The continuous change of θ means that the derivative of the bubble radius with respect to distance from the die, r', is a continuous function at the PET. Although we also desire v' to be a continuous function at the PET to get a smooth velocity profile, we cannot take it as a boundary condition; otherwise, the problem will be overspecified.

To carry out the simulation using the shooting method and starting from the die, the initial values of the stress components, $\sigma_{33}|_{die}$ and $p|_{die}$, must be specified. They are treated as two parameters in the present work. Luo and Tanner (1985) pointed out that the result of the simultation was not very sensitive to these two parameters. We assign $p|_{die} = 0$ (as Luo and Tanner did) and adjust $\sigma_{33}|_{die}$ to optimize the solution.

To find the alignment strength, values for the components of the Finger tensor are required. The Finger tensor at the die, $\mathbf{C}^{-1}(0, t')$, is assumed to be a unit tensor. In other words, all previous deformation history inside the die and the extruder is neglected and the polymer is assumed to be in a natural state when it leaves the die. This assumption is very rough. Since the polymer experiences a shearing stress inside the die, it cannot recover to the natural state immediately. However, since steady shear has little effect on the alignment strength of polymer chains, we may assign a value of zero to the alignment strength by assuming the Finger tensor is unit tensor. Future studies on the strain memory function inside the die may improve the simulation results.

System equations and boundary condition above the PET

At the PET, the constitutive model shifts from the liquidlike to the solidlike and the elastic strain components are obtained:

$$E_{11}|_p = \frac{\sigma_{11}|_p + p|_p}{2G_{eff}|_p} \tag{26}$$

$$E_{22}|_p = \frac{p|_p}{2G_{eff}|_p} \tag{27}$$

$$E_{33}|_p = \frac{\sigma_{33}|_p + p|_p}{2G_{eff}|_p} \tag{28}$$

where subscript p denotes the values at the PET.

Above the PET, the change of angle is expected to be very small due to the high effective modulus. We may then simplify the model equations by assuming $\theta' = 0$ such that Eq. 21 leads to

$$\sigma_{33} = \frac{r\Delta p}{h\cos\bar{\theta}} \tag{29}$$

The film contour angle above the freeze line, $\bar{\theta}$, is further assumed to be a small constant, slighly different from zero. These assumptions should be verified after the predicted bubble contour is found. The governing equations above the plastic transition are then found to be:

$$\sigma_{11} = 2G_{eff}(E_{11} - E_{22}) \tag{30}$$

$$p = 2G_{eff}E_{22} \tag{31}$$

$$\sigma_{33} = 2G_{eff}(E_{33} - E_{22}) \tag{32}$$

with

$$E_{11} = E_{11}|_p + \ln\frac{v}{v_p} \tag{33}$$

$$E_{33} = E_{22}|_p + \ln\frac{h}{h_p} \tag{34}$$

$$E_{33} = E_{33}|_p + \ln\frac{r}{r_p} \tag{35}$$

Equations 10, 23, and 29 to 31 represent the system equations above the PET, six equations for six unknowns, σ_{11}, σ_{33}, p, r, h, and T. These system equations are not differential equations and can be solved without boundary (initial) conditions except the energy equation, Eq. 23. Temperature at the plastic transition point is used in conjunction with Eq. 23 to solve for temperature profile above the plastic transition.

Results and Discussion

Very few data are available in the literature on film blowing of amorphous polymers. We, like Luo and Tanner (1986) and Cain and Denn (1988), use the experimental data of Gupta (1981), which is probably the only available data on amorphous polymers. Since the bubble radius, velocity profile, and temperature profile were all simultaneously measured and the resin, a product of Dow Chemical Co. was well characterized, the polystyrene resin data will provide some insight. This can only be considered to be a partial evaluation because the data at best extend only to the freeze line. Although typical industrial blow-up ratios are 2.5 to 8.0 for amorphous polymers, the maximum reported blow-up ratio in these data is 1.8. We will test the

model on only those data with a reported blow-up ratio greater than one (runs 17–20).

Gupta (1981) reported the temperature-dependent modulus and viscosity of the sample to be:

$$G = 8 \times 10^4 + (393 - T) \times 10^3 \text{ Pa} \tag{36}$$

$$\eta = 8.8 \times 10^4 \exp\left[18{,}904\left(\frac{1}{T} - \frac{1}{443}\right)\right] \text{Pa} \cdot \text{s} \tag{37}$$

Previous investigators modified some of these values in their attempts to fit the blown film simulation to the data of Gupta. Both Luo and Tanner, and Cain and Denn increased the modulus that Gupta reported by a factor of 2.5 when incorporating the data in their simulations. We used values for the modulus that were 1.51, 1.636, and 1.649 times larger than reported value for runs 18, 19, and 20, respectively. We were not successful in simulating Gupta's run 17 without making major modifications in the process parameters. The simulation results for this run are not included in the paper. For viscosity, we used the same expression given by Gupta, Eq. 37. Previous investigators also altered the viscosity equation; for example, Luo and Tanner seemed to use a viscosity four times larger than Gupta's, according to Eqs. 39 and 49 in their paper. The equilibrium yield stress and its temperature dependence were not reported in Gupta's study. They have been treated as two parameters in our simulation. This of course adds to the adjustable parameters. We use:

$$Y = 1 \times 10^{-15} \exp\left(\frac{2 \times 10^4}{T}\right) \text{Pa} \tag{38}$$

where the activation energy of yield is assumed to be similar to that of viscosity. It should be pointed out that these parameters were not adjusted for each run, and in fact the simulation result is not very sensitive to the value of the equilibrium yield stress. Varying the yield stress over a range of ±50% may cause the predicted PET to move up or down with respect to the die without much change in bubble shape if other parameters are slightly adjusted.

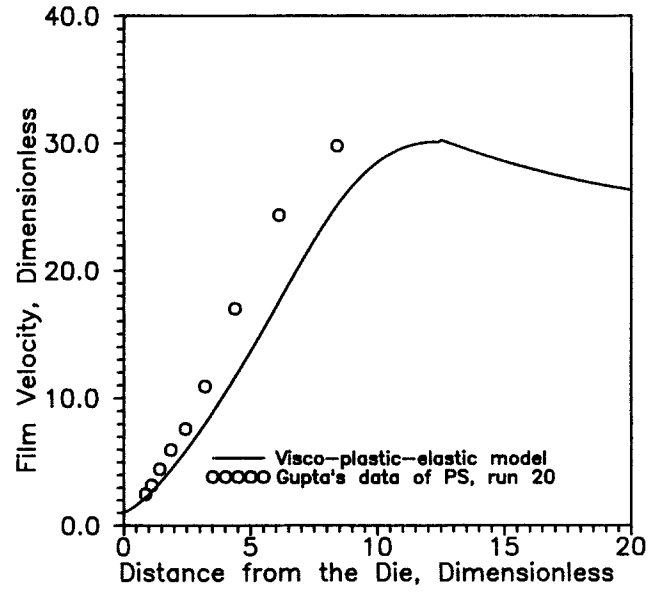

Figure 4b. Predicted film velocity.

The hardening constant, C_h, defined in Eq. 5, is another parameter. We have assigned a value of 0.06 to it in the simulation of Gupta's data, and find that it produces a fit. The hardening constant is also not adjusted with the run number.

Figures 4a, 4b, and 4c are presented as a comparison of the measured and the predicted bubble shape, velocity profile, and temperature profile for Gupta's run 20. This set of data was used by both Luo and Tanner, and Cain and Denn. The observation that the bubble radius initially decreases then rapidly increases and finally levels off is fairly well predicted. In our simulation, above the plastic transition, the bubble radius is not predicted to collapse to zero as was the case for the liquidlike models. Instead, the radius increases slowly at a decreasing rate and

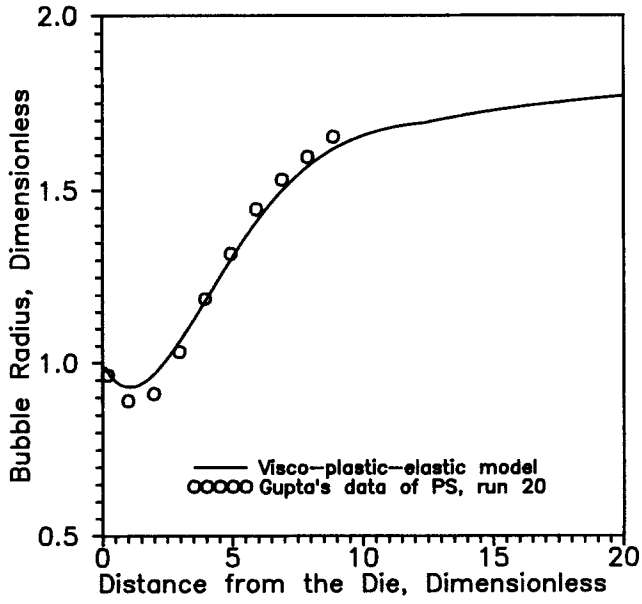

Figure 4a. Predicted bubble radius.

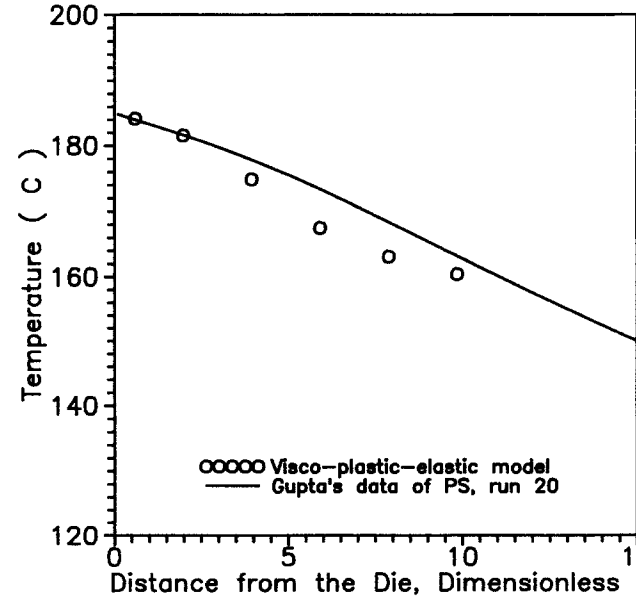

Figure 4c. Predicted temperature profile.

approaches an essentially straight bubble contour from the conventional freeze line up to the nips. Similarly good simulation results are produced for runs 18 and 19. It appears that the predicted film velocity is continuous at the PET but its first-order derivative is not continuous and the sign of the second-order derivative is opposite below and above the PET. This is due to the nature of the step functions of the constitutive equation; this model cannot guarantee consistency in the derivatives of velocity when shafting the governing equations.

In previously reported simulations, Luo and Tanner, and Cain and Denn, altered the process parameters in order to obtain a fit to the data when evaluating their models. In contrast, we use the experimentally reported values of measured take-up force and inflation pressure in all simulations (runs 18–20). The heat transfer coefficient is assumed to be a constant, 5.4 $W/m^2 \cdot K$, which is higher than 4 $W/m^2 \cdot K$ used by Luo and Tanner, and 1.6 $W/m^2 \cdot K$ by Cain and Denn. Even then, the predicted temperature does not decrease fast enough to fit the data, Figure 4c. The temperature at the PET for runs 18, 19, and 20 is at about 147, 156, and 158°C, respectively. In all of these cases, the PET's are at temperatures well above the reported glass transition temperature of 93 to 100°C for polystyrene, and their respective positions are close to the freeze line heights reported by Gupta.

The parameters which we adjusted in the simulation with the number of samples are initial angle of the film contour, initial hoop stress, and a factor to modify modulus, C_G

$$G = C_G[8 \times 10^4 + (393 - T) \times 10^3] \text{ Pa} \qquad (39)$$

Their values are listed in Table 1.

Unlike the bubble radius and temperature, the simulated velocity is not a monotonic function and it tends to increase in the vicinity of the plastic transition before decreasing to an equilibrium value above the freeze line. The simulated results, for example in Figure 4b, are found to differ from the experimental data by up to about 10%. It follows that the film is predicted to shrink in the axial direction. The combined effect of the changes in bubble radius and velocity above the plastic transition results

Table 1. Parameters in the Simulation Using the Current Model

Parameter	Run 18	Run 19	Run 20
C_G	1.51	1.636	1.649
$\theta\|_{z=0}$	−0.16	−0.12	−0.16
$\left.\frac{\sigma_{33}}{\sigma_{11}}\right\|_{z=0}$	0.54	0.45	0.42
F_z, g	226	240	217
Δp, kPa	0.186	0.196	0.216
$\dot{m}$, kg/s	0.262×10^{-3}	0.239×10^{-3}	0.290×10^{-3}
$T\|_{z=0}$, °C	185	184	185

Parameters Held Constant for All Runs

Hardening constant, $C_h = 0.06$
Heat transfer coefficient, $U = 5.4$ kW/m$^2 \cdot$ K
Film thickness at die, $h_0 = 0.1016$ cm
Bubble radius at die, $r_0 = 1.27$ cm
Film density, $\rho = 1.05$ g/cm^3
Heat capacity, $c_p = 1{,}910$ J/kg $\cdot$ K

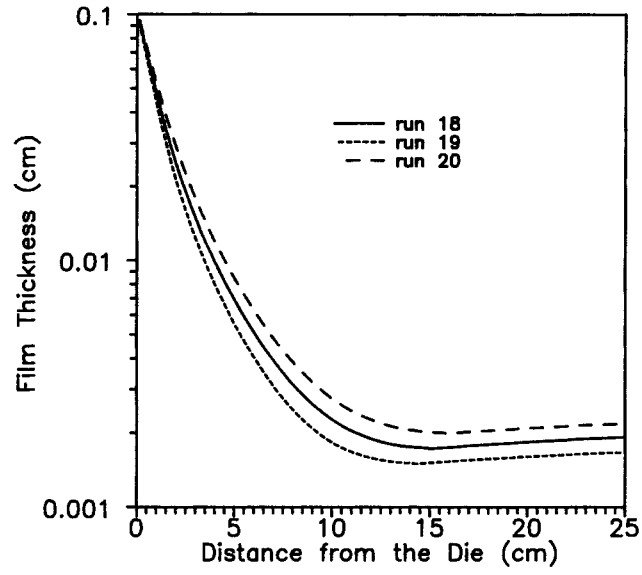

Figure 5. Predicted film thickness.

in a slightly thicker film at the nip rolls than that at the freeze line, as shown in Figure 5. It would be of interest to test this prediction on the blown film line. However, the reported data stop at or below the freeze line and to accomplish this we would require an on-line thickness gauge that is temperature independent to check the thickness as a function of position. Such an instrument is not available at this time.

In analyzing the simulation results, it would be of interest to see how the the structure memory function, ζ, develops as the material is stretched from the die to the nip rolls, since this information may ultimately correlate with the physical properties of the film. Figure 6 illustrates the profile of the structure memory function. It is similar in shape to the velocity profile. The results indicate that the value of the structure memory function rapidly increases from the die to the PET, and then softens a little. If this can be measured experimentally, it will be

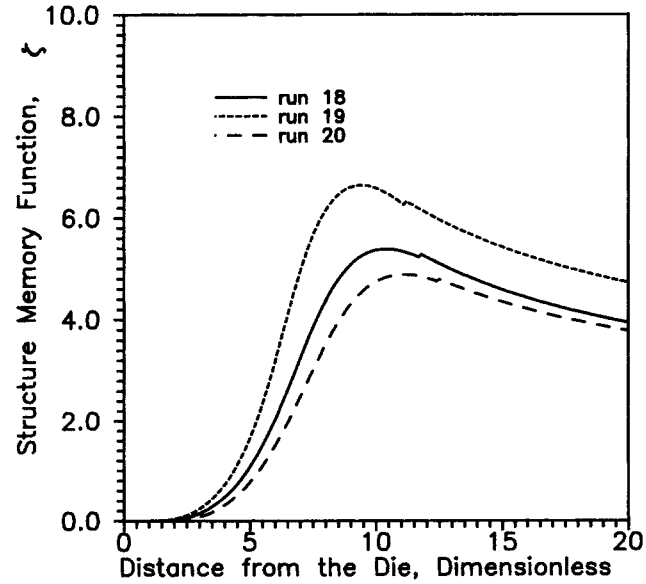

Figure 6. Structure memory function, ζ, profiles.

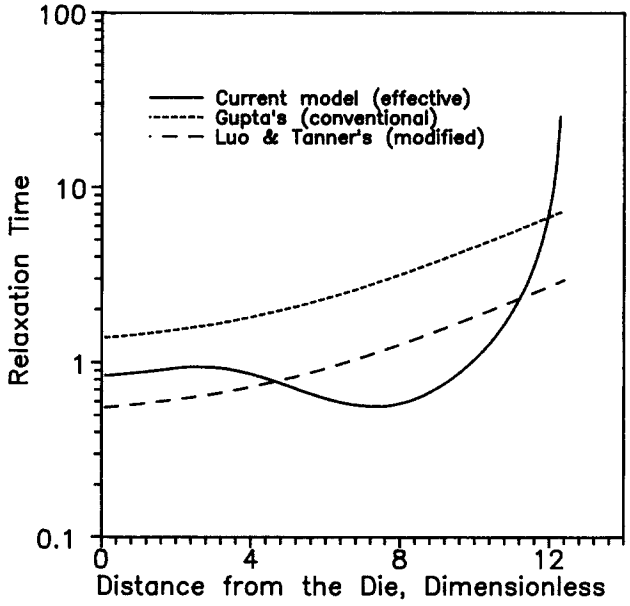

Figure 7. Relaxation time.

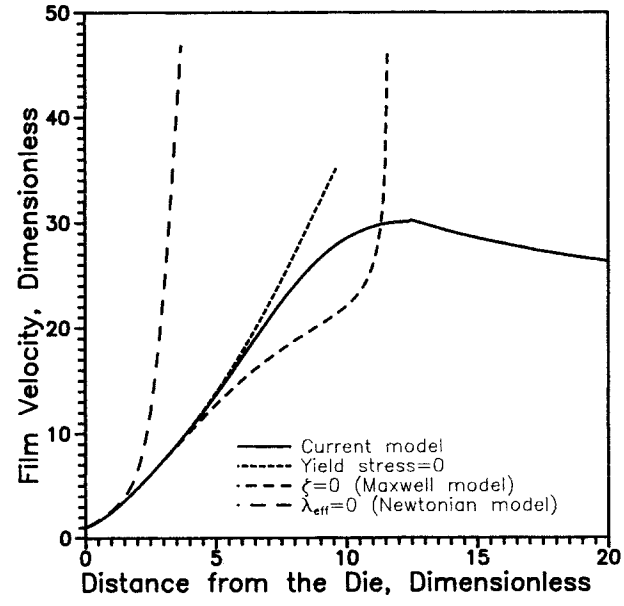

Figure 8b. Influence of parameters on predicted film velocity.

a significant prediction, since the quality of the film may be related to the structure.

From a rheological point of view, the change in relaxation time should be of interest when compared with other definitions. Our effective relaxation time, defined in Eq. 7, is plotted with the conventional relaxation time, defined as $\lambda = \eta/G$ (using Gupta's data), and modified relaxation time, defined as $\lambda = \eta/2.5G$ (using Luo and Tanner's modified modulus of Gupta). Figure 7, for run 20, is representative of the relaxation times used in the simulations. The conventional relaxation time and the modified relaxation time are monotonic functions of the distance from the die since they are monotonic functions of temperature, and temperature decreases almost linearly as the distance from the die increases. In contrast, the predicted effective relaxation time displays a complex behavior, increasing and decreasing and then increasing again very rapidly. At the PET, the effective relaxation time goes to infinity. The effective relaxation is, by our definition, not only a function of temperature but also a function of stress and the structure memory function, which depends on strain and strain rate.

Introducing the concepts of the strain hardening and yield stress also introduces parameters into the model. It is of interest to examine the utility of those parameters by removing them from the constitutive equation. The results of this exercise are presented graphically in Figures 8a–c. The results labeled *Current model* are the same results we presented previously for run 20 of Gupta. One of the key changes that we incorporated in the

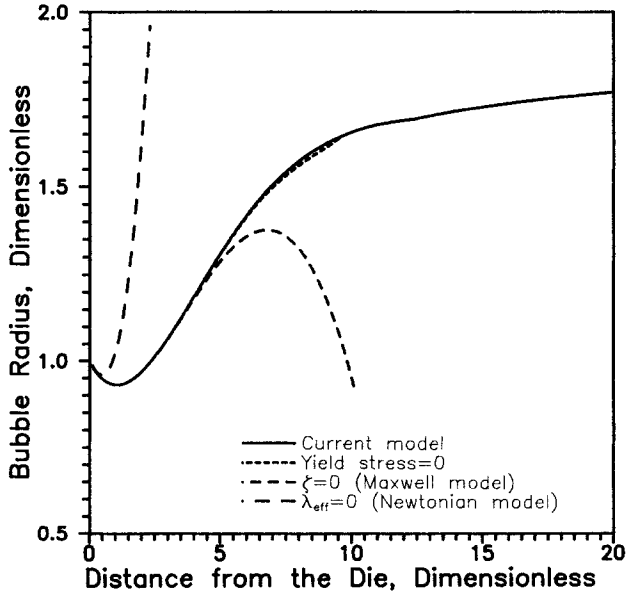

Figure 8a. Influence of parameters on predicted bubble radius.

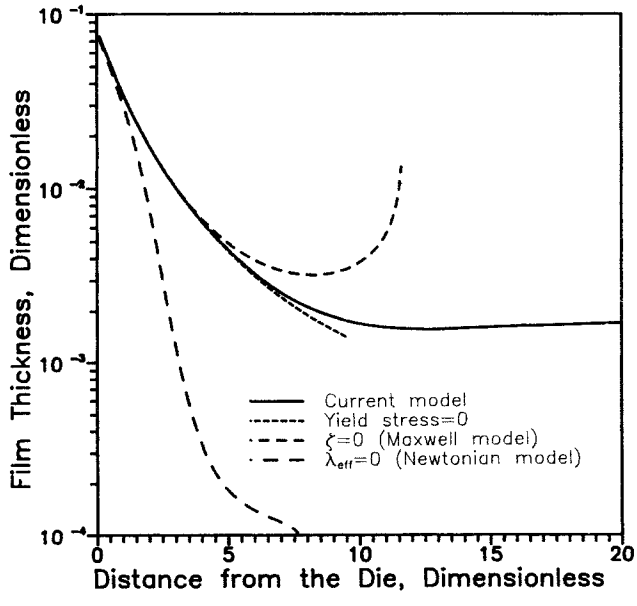

Figure 8c. Influence of parameters on predicted film thickness.

Maxwell model is yield stress. The argument as to the existence of the yield stress leads us to examine the effect of the yield stress on the simulation result. When we set the yield stress equal to zero, a similar bubble radius is predicted while quite different film thicknesses and velocities are produced; the film thickness approaches zero and the velocity appears to be increasing rapidly and appears to be unbounded. This is not proof of the existence of yield stress, but it shows that yield stress, as an engineering tool, does improve the simulation. These results suggest a mechanistic response relating the rheology to the process variables. When the yield stress was removed but the strain hardening effect on the modulus was retained in the simulation, the radius was found to follow the experimental result while the velocity was found to deviate from the observed process characteristics up to the reported freeze line. This suggests that the bubble radius is dominated by the modulus of the material as simulated by the constitutive equation. However, the velocity seems to be most closely related to the viscous component in the constitutive equation blow the freeze line or the PET. The influence of yield stress on the film velocity through effective viscosity appears to cause the film velocity to approach a limit as the effective yield stress increases rapidly due to the decreasing temperature and increasing orientation.

Another key change that we introduced into the Maxwell model is a so-called structure memory function, ζ. This parameter, when combined with the modulus and yield stress, is used to indicate the effect of molecular orientation on the rheological properties. We remove this change by setting the strain hardening constant, C_h, equal to zero in Eq. 5. This reduces the constitutive equation to the conventional Maxwell model. We observe that none of the predicted results, bubble radius, film thickness, or velocity even qualitatively resemble Gupta's data if $\zeta = 0$, as shown in Figures 8a–c. The radius goes through a maximum, the film thickness goes through a minimum, and the velocity appears to be unbounded.

As we pointed our previously, our model reduces to the Newtonian model if the effective relaxation time is equal to zero. In Figures 8a–c we plot the predictions using the same set of parameters except for $\lambda_{eff} = 0$. It appears that the bubble radius and the film velocity increase very rapidly and are unbounded. Adjusting the magnitude of the viscosity or the operating parameters such as inflation pressure will predict a collapsing of the bubble above the freeze line.

Summary

The above analysis has produced results that are consistent with our goals. First, we have a model that allows a natural shift from liquidlike to solidlike behavior in the vicinity of the freeze line. Second, the rheological model used leads to the use of unaltered process parameters in the simulation. The proposed viscoplastic-elastic model incorporates the strain hardening phenomenon through an argument of the alignment strength. An effective relaxation time is defined to characterize the transient and thermodynamically irreversible nature of the blown film process. The model is quantitatively consistent with the literature data below the plastic transition and qualitatively in agreement with desired results above the plastic transition, that is, approaching a constant radius and velocity as the material moves toward the nip rolls. We feel that this approach has merit because for the first time the actual measurable process parameters were used in the entire simulation from the die to a point well beyond the reported freeze line, with results that compare well with the limited literature data.

Acknowledgment

Thanks are due to the General Electric Company for providing financial support to B. Cao. We wish to thank Paul Sweeney for many helpful suggestions during the development of this investigation.

Notation

$\mathbf{C}$ = Cauchy-Green tensor
$\mathbf{C}^{-1}$ = Finger tensor, Eq. 15
C_G = modulus constant, Eq. 39
C_h = hardening constant, Eq. 5
C_p = heat capacity, $J/kg \cdot K$
$\mathbf{D}$ = deformation rate tensor, Eq. 9
$\mathbf{E}$ = strain tensor, Eq. 14
F_z = take-up force, g
G = modulus, Pa
h = film thickness, cm
I_1 = first invariant of Finger tensor
I_2 = second invariant of Finger tensor
$\dot{m}$ = polymer flow rate, K_g/s
p = thermodynamic pressure, Pa
Δp = inflation pressure, Pa
r = bubble radius, cm
R_H = principle radius of curvature, Eq. 13
R_L = principle radius of curvature, Eq. 12
t = time, s
t' = time, s
T = temperature, K or °C
T_a = ambient temperature, K
U = heat transfer coefficient, $W/m^2 \cdot K$
v = film velocity, cm/s
Y = yield stress, Pa
z = distance from the die, cm

Greek letters

δ_{ij} = unit tensor
ϵ = emissivity, Eq. 23
ζ = structure memory function, Eq. 5
η = viscosity, $Pa \cdot s$
θ = axial angle of the bubble contour, natural value
λ = relaxation time, s
λ = Stefan-Boltzmann constant, $5.67 \times 10^{-8} W/m^2 \cdot K^4$
ξ = coordinate measure, cm
ρ = density, g/cm^3
σ = total stress tensor, Pa
τ = stress tensor, Pa
ψ = alignment strength, Eq. 3
Π_D = second invariant of deformation rate tensor
Π_τ = second invariant of stress tensor

Subscripts

0 = value at the die
eff = effective value
f = value at the freeze line
p = value at the plastic-elastic transition

Literature Cited

Beatty, C. L., and J. L. Weaver, "Effect of Temperature on the Compressive Stress-Strain Properties of Polystyrene," *Polym. Eng. Sci.*, **18**,1109 (1978).

Bird, R. B., R. C. Armstrong, O. Hassager, *Dynamics of Polymeric Liquids*, 419, Wiley, New York (1977).

Campbell, G. A., and B. J. Cao, "The Interaction of Crystallinity, Elastoplasticity, and a Two-Phase Model on Blown Film Bubble Shape," *Plastic Film & Sheet.*, **3**, 158 (1987).

Cao, B., and G. A. Campbell, "Air Ring Effect on Blown Film Dynamics," *J. Int. Polymer Process.*, **4**, 114 (1989).

Cao, B., P. Sweeney, and G. A. Campbell, "Simultaneous Surface and Bulk Temperature Measurement of Polyethylene During Film Blowing," SPE *ANTEC 35* (1989).
Cain, J. J., and M. M. Denn, "Multiplicities and Instabilities in Film Blowing," *Polym. Eng. Sci.*, **28,** 1527 (1988).
Chow, T. S., "Fundamental Relationship between the Nonequilibrium Glassy State and Yield Stress of Amorphous Polymers," *J. Polym. Sci. B, Polym. Phys.*, **25,** 137 (1987).
Giesekus, H., "A Simple Constitutive Equation for Polymer Fluids Based on the Concept of Deformation-Dependent Tensorial Mobility," *J. Non-Newtonian Fluid Mech.*, **11,** 69 (1982). *Rheol. Acta,* **5,** 29 (1966).
Gupta, R. K., "A New Nonisothermal Rheological Constitutive Equation and its Application to Industrial Film Blowing Process," Ph.D. Thesis, Univ. Delaware (1981).
Han, C. D., and J. Y. Park, "Studies on Blown Film Extrusion: II. Analysis of the Deformation and Heat Transfer Process," *J. Appl. Polym. Sci.*, **19,** 3257 (1975).
Hartmann, B., and R. F. Cole, Jr., "Tensile Yield in Poly(4-Methyl Pentene-1)," *Polym. Eng. Sci.*, **23,** 13 (1983).
Hartnett, J. P., and R. Y. Z. Hu, "The Yield Stress—An Engineering Reality," *J. Rheol.*, **33,** 671 (1989).
Hill, R., *The Mathematical Theory of Plasticity*, 19 Oxford, Clarendon Press (1950).
Kanai, T., and J. L. White, "Kinematics, Dynamics and Stability of the Tubular Film Extrusion of Various Polyethylenes," *Polym. Eng. Sci.*, **24,** 1185 (1984).
———, "Dynamics, Heat Transfer and Structure Development in Tubular Film Extrusion of Polymer Melts: A Mathematical Model and Predictions," *J. Polym. Eng.*, **5,** 135 (1985).
Larson, R. G., *Constitutive Equations for Polymer Melts and Solutions*, 146, 151, 197, Butterworth (1988).
Luo, X. L., and R. I. Tanner, "A Computer Study of Film Blowing," *Polym. Eng. Sci.*, **25,** 620 (1985).
Meissner, J., "Dynamics of Polymeric Liquids," *Rheol. Acta,* **10,** 230 (1971).
Pearson, J. R. A., and C. J. S. Petrie, "The Flow of a Tubular Film. Part 1. Formal Mathematical Representation," *J. Fluid Mech.*, **40,** 1 (1970a).
———, "The Flow of a Tubular Film. Part 2. Interpretation of the Model and Discussion of Solutions," *J. Fluid Mech.*, **42,** 1 (1970b).
———, "A Fluid-Mechanical Analysis of the Film-Blowing Process," *Plast. Polym.*, **38,** 85 (1970c).
Petrie, C. J. S., "Memory Effects in a Non-uniform Flow: A Study of the Behavior of Tubular Film of Viscoelastic Fluid," *Rheol. Acta,* **12,** 92 (1973).
———, "Mathematical Modeling of Heat Transfer in Film Blowing—A Case Study," *Plast. Polym.*, **44,** 259 (1974).
———, "A Comparison of Theoretical Predictions with Published Experimental Measurements on the Blow Film Process," *AIChE J.*, **21,** 275 (1975).
Phan, N. T., and R. I. Tanner, "A New Constitutive Equation Derived from Network Theory," *J. Non-Newtonian Fluid Mech.*, **2,** 353 (1977).
Wagner, M. H., "A Rheologic-Thermodynamic Process, Model of the Film Blowing Process," *Rheol. Acta,* **15,** 40 (1978).
———, Ph.D. Diss., Univ. Stuttgart (1978).
White, J. L., and A. B. Metzner, "Development of Constitutive Equations for Polymeric Melts and Solutions," *J. Appl. Polym. Sci.*, **8,** 1367 (1963).
Winter, H. H., "Modelling of Strain Histories for Memory Integral Fluids in Steady Axisymmetric Flows," *J. Non-Newtonian Fluid Mech.*, **10,** 157 (1982).

Manuscript received Aug. 4, 1989, and revision received Dec. 4, 1989.